Bioresource Technology 109 (2012) 148–153

Contents lists available at SciVerse ScienceDirect

Bioresource Technology

journal homepage: www.elsevier.com/locate/biortech

Thermal decomposition of wood: Influence of wood components and cellulose crystallite size

Matheus Poletto [a,b,*], Ademir J. Zattera [b], Maria M.C. Forte [a], Ruth M.C. Santana [a]

[a] Programa de Pós-graduação em Engenharia de Minas, Metalúrgica e de Materiais, Universidade Federal do Rio Grande do Sul, Av. Bento Gonçalves 9500, 91501-970 Porto Alegre, RS, Brazil
[b] Laboratório de Polímeros, Universidade de Caxias do Sul, Rua Francisco Getúlio Vargas 1130, 95070-560 Caxias do Sul, RS, Brazil

ARTICLE INFO

Article history:
Received 10 October 2011
Received in revised form 25 November 2011
Accepted 28 November 2011
Available online 21 January 2012

Keywords:
Wood
Cellulose
Crystallite size
Thermal analysis
X-ray diffractometry

ABSTRACT

The influence of wood components and cellulose crystallinity on the thermal degradation behavior of different wood species has been investigated using thermogravimetry, chemical analysis and X-ray diffraction. Four wood samples, *Pinus elliottii* (PIE), *Eucalyptus grandis* (EUG), *Mezilaurus itauba* (ITA) and *Dipteryx odorata* (DIP) were used in this study. The results showed that higher extractives contents associated with lower crystallinity and lower cellulose crystallite size can accelerate the degradation process and reduce the wood thermal stability. On the other hand, the thermal decomposition of wood shifted to higher temperatures with increasing wood cellulose crystallinity and crystallite size. These results indicated that the cellulose crystallite size affects the thermal degradation temperature of wood species.

1. Introduction

Biomass has been recognized as a potential renewable energy and a substitute for the declining supply of fossil fuel resources (Kim et al., 2010a; Wongsiriamnuay and Tippayawong, 2010; Shen and Gu, 2009). Common sources of biomass include several kinds of wood, agricultural crops and natural fibers (Wongsiriamnuay and Tippayawong, 2010). The interest in biomass as an alternative energy is increasing as a result of it continuous regeneration. On the other hand, biomass in a fiber or particulate form has been used as a reinforcing filler in thermoplastic composite materials (Poletto et al., 2011a; Ashori and Nourbakhsh, 2010; Liu et al., 2009). These lignocellulosic materials are in general suitable for addition to reinforced plastics due to their relative high strength and stiffness, low cost, low density, low CO_2 emission and biodegradability besides being annually renewable (Nachtigall et al. 2007; Araújo et al., 2008). However, they present limitations such as moisture adsorption and low thermal stability (Araújo et al., 2008; Poletto et al., 2010).

Wood is a polymeric composite, which essentially contains cellulose, hemicellulose, lignin and extractives. Wood degradation takes place at a relatively low temperature, around 200 °C (Araújo et al., 2008; Poletto et al., 2010). As a result, wood is subjected to thermal degradation during composite processing with the majority of the thermoplastic polymers (Liu et al., 2009). The degradation of wood resulting from high processing temperatures may lead to undesirable properties, such as odor and browning, along with a reduction in mechanical properties of the developed composite (Liu et al., 2009; Shebani et al., 2009). Therefore, it is of practical significance to understand and predict the thermal decomposition process of wood so that this knowledge can aid to better design a composite-obtaining process and estimate the influence of the thermal decomposition of wood on composite properties (Yao et al., 2008).

Due to the complexity of the thermal decomposition reactions of wood, extensive researches have determined individual behaviors of the main wood components. Órfão et al. (1999) and Órfão and Figueiredo (2001) introduced three independent reaction models to describe the pyrolysis kinetics of some lignocellulosic materials, while Branca et al. (2005) and Di Blasi (2008) used three parallel reactions to describe the fast pyrolysis process of wood. Grønli et al. (2002) showed a devolatilization mechanism of hardwoods and softwoods consisting of three parallel reactions resulting from the degradation of the three main components of wood.

A considerable amount of work has been reported on the study of wood decomposition as mentioned above. However, the literature lacks works on the influence of wood components and wood cellulose crystallinity on the degradation of wood species. In this

* Corresponding author at: Programa de Pós-graduação em Engenharia de Minas, Metalúrgica e de Materiais, Universidade Federal do Rio Grande do Sul, Av. Bento Gonçalves 9500, 91501-970 Porto Alegre, RS, Brazil. Tel.: +55 54 3218 2108; fax: +55 54 3218 2253.
E-mail address: mpolett1@ucs.br (M. Poletto).

0960-8524/$ - see front matter © 2012 Published by Elsevier Ltd.
doi:10.1016/j.biortech.2011.11.122

context, this work has evaluated how the wood components and wood cellulose crystallinity influence wood thermal stability. Four different wood species from Brazil were investigated using chemical analysis, X-ray diffraction and thermogravimetric analysis.

2. Methods

2.1. Materials

The wood flour samples used in this study were obtained from wastes of the Brazil lumber industry. The species investigated were *Pinus elliottii*, *Eucalyptus grandis*, *Mezilaurus itauba* and *Dipteryx odorata*. Samples having particle size between 200 and 300 μm were dried in a vacuum oven at 105 °C for 24 h before the thermogravimetric analysis.

2.2. Chemical analysis

Benzene and absolute ethanol purchased from Vetec Chemical were used to determine the amount of organic extractives in the wood samples. Sulphuric acid purchased from Vetec Chemical was used for insoluble lignin determination. The wood extractives were eliminated from wood via Soxhlet extraction in triplicate using: ethanol/benzene and ethanol and hot water according to the Tappi T204 cm-97 standard. The Klason lignin content was determined according to the Tappi T222 om-02 standard. The determination of the ash content was carried out at 600 °C for 1 h in a muffle furnace, based on Tappi T211 om-02. The holocellulose content (cellulose + hemicellulose) was determined by difference.

2.3. X-ray diffraction (XRD)

X-ray diffractograms were collected using a sample holder mounted on a Shimadzu diffractometer (XRD-6000), with monochromatic Cu Kα radiation ($\lambda = 0.1542$ nm), the generator operating at 40 kV and 30 mA. Intensities were measured in the range of $5 < 2\theta < 35°$, typically with scan steps of 0.05° and 2 s/step (1.5°min^{-1}). Peak separations were carried out using Gaussian deconvolution. After deconvolution it is possible to calculate and compare several parameters. The *d*-spacings were calculated using the Bragg equation [17,18].

The crystalline index (Eq. (1)), proposed by Hermans et al. (Wada and Okano, 2001; Popescu et al., 2011) is:

$$\mathrm{Cr\cdot I\cdot} = \frac{A_{cryst}}{A_{total}} \quad (1)$$

where Cr.I. is the crystalline index, A_{cryst} is the sum of crystalline band areas, and A_{total} is the total area under the diffractograms.

The second approach used to determine the crystalline index (Eq. (2)) was the empirical method proposed by Segal et al. (1959) (Wada and Okano, 2001; Gümüskaya et al., 2003):

$$\mathrm{C\cdot I\cdot} = \frac{I_{002} - I_{am}}{I_{002}} \times 100 \quad (2)$$

The apparent crystallite size (*L*) (Eq. (3)) was calculated using the Scherrer equation (Popescu et al., 2011):

$$L = \frac{K * \lambda}{\beta * \cos\theta} \quad (3)$$

where *K* is a constant of value 0.94, λ is the X-ray wavelength (0.1542 nm), β is the half-height width of the diffraction band and θ is the Bragg angle corresponding to the (200) plane.

The surface chains occupy a layer approximately 0.57 nm thick so the proportion of crystallite interior chains (Popescu et al., 2011; Davidson et al., 2004) is:

$$X = \frac{(L - 2h)^2}{L^2} \quad (4)$$

where *L* is the apparent crystallite size for the reflection of plane (200), and $h = 0.57$ nm is the layer thickness of the surface chain.

2.4. Thermogravimetric analysis (TGA)

The thermogravimetric analysis (TGA50 – Shimadzu) was carried out under N_2 atmosphere with a purge gas flow of 50 cm^3 min^{-1} from 25 to 800 °C. Approximately 10 mg of each sample was used. The heating rate of the analysis was 10 °C min^{-1}.

3. Results and discussions

3.1. Chemical composition of wood species

In order to determine the effect of the chemical composition of wood species under study on the wood thermal stability the amount of holocellulose, lignin and extractives was determined for all samples. The initial wood degradation temperature is expected to be related to the heat stability of the individual wood components and differences in thermal stability among wood species can be attributed to the variation in chemical composition (Poletto et al., 2010; Shebani et al., 2008). On the other hand, the fundamental differences among wood species are found in the types, size, proportions, pits and arrangements of the different cells that compose wood (Popescu et al., 2011). These differences might affect the crystallinity and crystallite size of the wood species with impacts on wood thermal stability.

The results for the chemical composition of the wood species studied are presented in Table 1. The holocellulose and lignin contents were higher for the EUG and PIE species than for the DIP and ITA species. The PIE had the highest lignin content around 34% while ITA had the lowest, 28%. The holocellulose content of wood is generally around 60–70%, while the lignin is usually in the range of 20–35% (Rowell, 2005; Klyosov, 2007). However, ITA and DIP contain three times more extractives than EUG and PIE. In general, the extractives content varies between 2% and 5% but it can exceed 15% in some wood species (Shebani et al., 2008; Klyosov, 2007). The ash content of the DIP species was higher than that of the other species studied and this value is probably associated with higher amounts of mineral salts in this wood species than in the other species evaluated. The inorganic content of a wood species is usually referred to as its ash content, which is an approximate measure of its mineral salts and other inorganic matters content. It normally varies between 0.2% and 0.5% in wood (Rowell, 2005; Klyosov, 2007), but tropical species often exceed this range (Branca and Di Blasi, 2003; Hon and Shiraishi, 2001).

Table 1
Chemical composition of the investigated wood species.

Wood species	Holocellulose (%)	Lignin (%)	Extractives (%)	Ash (%)
Eucalyptus grandis (EUG)	62.7 ± 1.4	32.1 ± 1.0	4.1 ± 0.2	1.1 ± 0.3
Pinus elliottii (PIE)	61.2 ± 1.1	33.8 ± 1.0	4.5 ± 0.1	0.8 ± 0.1
Dipteryx *odorata* (DIP)	57.1 ± 0.6	30.4 ± 0.4	11.1 ± 0.1	1.5 ± 0.2
Mezilaurus itauba (ITA)	57.8 ± 1.0	28.0 ± 0.3	13.6 ± 0.7	0.7 ± 0.1

3.2. X-ray diffraction

The X-ray diffraction is a method used generally to evaluate the degree of crystallinity in several materials. Among wood components, only cellulose is crystalline, while hemicellulose and lignin are non-crystalline (John and Thomas, 2008). The free hydroxyl groups present in the cellulose macromolecules are likely to be involved in a number of intramolecular and intermolecular hydrogen bonds, which may give rise to various ordered crystalline arrangements (Popescu et al., 2011; Poletto et al., 2011b).

Fig. 1 shows the X-ray diffractograms of the wood samples studied. In order to examine the intensities of the diffraction bands, establish the crystalline and amorphous areas more exactly and determine the crystallite sizes the diffractograms were deconvoluted using Gaussian profiles. The peak intensities and peak broadening differ from one species to another. The more pronounced difference occurs at the peak range between 21.90° and 22.20° 2θ reflection assigned with a crystallographic plane of cellulose. The peak area at 21.90–22.20° 2θ reflection follow the sequence DIP > ITA > EUG > PIE, as can be seen in Fig. 1.

Crystallographic planes are labeled according to the native cellulose structure as described by Wada et al. (2001). After deconvolution, all diffractograms show the 14.8–15.3° 2θ reflection assigned to the $(1\bar{1}0)$ crystallographic plane, the 16.20–16.30° 2θ reflection assigned to the (110) crystallographic plane, the 18.30–18.40° 2θ reflection assigned to the amorphous phase and the 21.90–22.20° 2θ reflection assigned to the (200) crystallographic plane of cellulose I (Popescu et al., 2011; Wada et al., 2001). Fig. 2 shows a model to represent the cellulose chains and the crystallographic planes described above.

Wood cellulose is known to be a composite of two distinct crystalline structures, namely I_α and I_β. The I_α and I_β structures are assigned to triclinic and monoclinic unit cells, respectively (Poletto et al., 2011b; Wada et al., 2001). The d-spacings of wood celluloses calculated from X-ray diffractometry profiles were 0.579–0.599 nm for $d_{(1\bar{1}0)}$ and 0.542–0.554 nm for $d_{(1\,1\,0)}$, as can be seen in Table 2. These figures indicated that wood cellulose samples used in this study are all I_β-type cellulose (Wada and Okano, 2001; Wada et al., 2001). These values are significantly different from the d-spacings of the I_α-rich type celluloses, 0.610–0.617 nm for $d_{(1\bar{1}0)}$ and 0.530–0.541 nm for $d_{(1\,1\,0)}$ (Kim et al., 2010a,b). These data support previous results from diffraction methods stating that the monoclinic structure (I_β) is dominant in wood cellulose (Wada et al., 2001; Kim et al., 2010a,b).

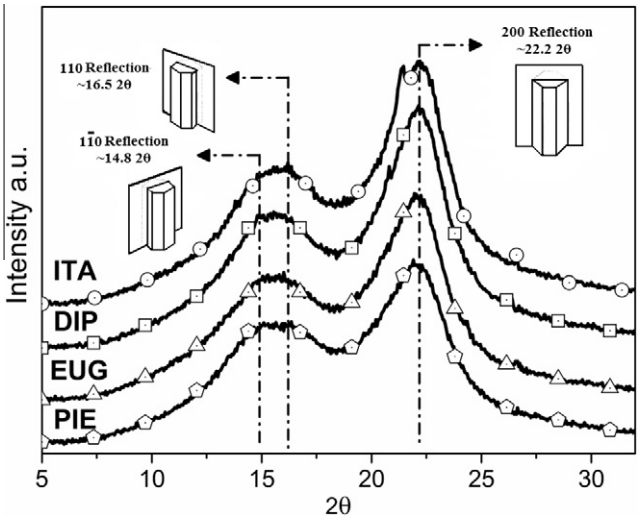

Fig. 1. X-ray diffractograms of wood species studied with corresponding crystal planes, adapted from (Howell, 2008), and most common 2θ values.

The degree of cellulose crystallinity is one of the most important crystalline structure parameters. The rigidity of cellulose fibers increases and their flexibility decreases with increasing ratio of crystalline to amorphous regions (Gümüskaya et al., 2003). The crystallinity index calculated according to the Hermans (Eq. (1)) and Segal methods (Eq. (2)) showed that the crystallinity of the DIP and ITA species was higher than that of EUG and PIE, as presented in Table 3. These differences are confirmed when the values of the crystallite size along the three crystallographic planes are taken into consideration. Crystallinity indices increased with increasing crystallite sizes because the crystallites surface corresponding to amorphous cellulose regions diminished (Kim et al., 2010a,b). These results indicated that DIP and ITA contain a more ordered cellulose structure than EUG and PIE.

The values of *X* were used as estimates of the fraction of cellulose chains contained in the interior of the crystallites (Newman, 1999). Once again, DIP and ITA species showed higher values than EUG and PIE. This result confirms that DIP and ITA wood species contain much more cellulose chains in a highly organized form in the interior of the cellulose crystallite. This can lead to higher hydrogen bond intensity among neighboring cellulose chains

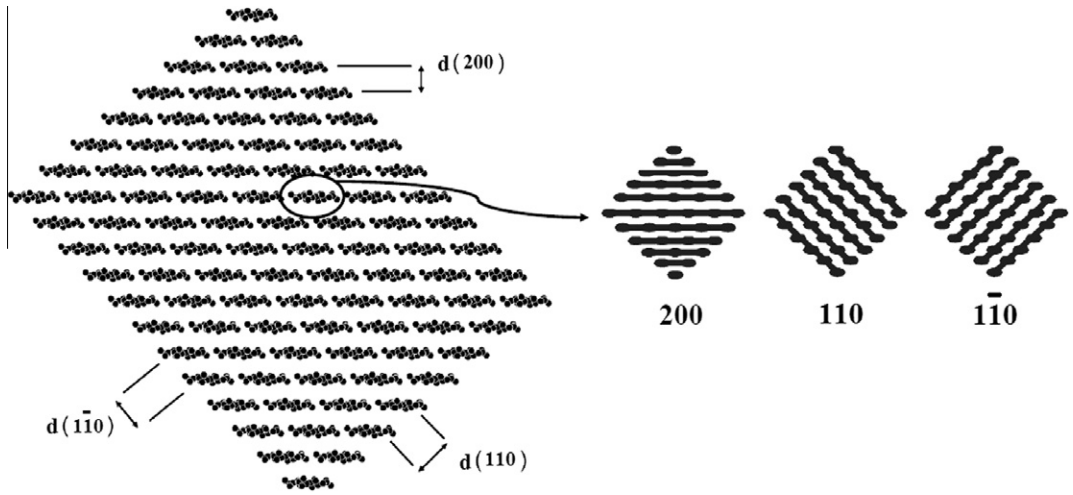

Fig. 2. Model used to represent cellulose chains (left), showing the d-spacings along the cellulose structure, adapted from (Newman, 2008). Lines indicated the crystallographic planes in native cellulose (right), each ellipse represents a chain normal to the paper, adapted from (Newman, 1999).

Table 2
Band position (2θ) and d-spacings of crystalline and amorphous cellulose regions for the wood samples studied.

Wood species	$(1\bar{1}0)$		(110)		Amorphous	(200)	
	2θ	d (nm)	2θ	d (nm)	2θ	2θ	d (nm)
Eucalyptus grandis (EUG)	15.30	0.579	16.01	0.554	18.30	21.95	0.405
Pinus elliottii (PIE)	15.10	0.587	16.35	0.542	18.40	21.90	0.406
Dipteryx *odorata* (DIP)	14.91	0.595	16.30	0.544	18.40	22.15	0.402
Mezilaurus itauba (ITA)	14.80	0.599	16.20	0.547	18.35	22.20	0.401

Table 3
Parameters obtained from the XRD analysis of the wood samples studied.

Wood species	L $(1\bar{1}0)$ (nm)	L (110) (nm)	L (200) (nm)	Cr.I.	C.I.	X
Eucalyptus grandis (EUG)	1.72	2.29	2.11	34.4	49.3	0.21
Pinus elliottii (PIE)	1.71	2.44	1.92	34.1	43.4	0.17
Dipteryx *odorata* (DIP)	1.97	2.30	2.18	43.0	55.7	0.23
Mezilaurus itauba (ITA)	1.81	2.13	2.23	37.8	52.7	0.24

result in a more packed cellulose structure besides higher crystallinity. On the other hand, the thermal stability of cellulose was found to depend mainly on its crystallinity index, crystallite size and degree of polymerization (Poletto et al., 2011b; Kim et al., 2010b; Nada et al., 2000).

3.3. Thermogravimetric analysis

Fig. 3 shows the results of the thermogravimetric analysis performed on the different wood species. Fig. 3(a) gives the percentage of weight loss as a function of temperature, while Fig. 3(b) presents the derivative thermogravimetric curves. Water loss is observed around 100 °C, and further thermal degradation takes place as a two-step process. In the first step, the degradation of hemicellulose takes place at around 300 °C and a slight shoulder in the DTG curve can be seen in Fig. 3(b) for all wood species studied. At around 350 °C the main degradation of cellulose occurs and a prominent peak appears at the temperature corresponding to the maximum decomposition rate. According to Kim et al. (2006) the depolymerization of hemicellulose occurs between 180 and 350 °C, the random cleavage of the glycosidic linkage of cellulose between 275 and 350 °C and the degradation of lignin between 250 and 500 °C. The higher activity of hemicellulose in thermal decomposition might be attributed to its chemical structure (John and Thomas, 2008; Yang et al., 2006). Hemicellulose has a random amorphous structure and it is easily hydrolyzed (John and Thomas, 2008; Yang et al., 2006). In contrast, the cellulose molecule is a very long polymer of glucose units, and its crystalline regions improve the thermal stability of wood (Yang et al., 2006). Lignin is different from hemicellulose and cellulose because it is composed of three kinds of benzene-propane units, being heavily cross-linked and having very high molecular weight (John and Thomas, 2008; Yang et al., 2006). The thermal stability of lignin is thus very high, and it is difficult to decompose (Yang et al., 2006).

As can be seen in detail in Fig. 3(a) at temperatures around 180–190 °C the ITA wood shows a more significant weight loss. This behavior might be associated with the highest content of extractives in this wood, around 14% as presented in Table 1. Extractives are compounds of lower molecular mass as compared to cellulose, and can promote ignitability of the wood at lower temperatures as a result of their higher volatility and thus accelerate the degradation process. In this way, the degradation of one component may accelerate the degradation of the other wood components. Grønli et al. (2002) and Shebani et al. (2008) observed that wood degradation at low temperatures is usually associated with extractive decomposition. On the other hand, the individual chemical components of wood behave differently if they are isolated or intimately combined within each single cell of the wood structure (Popescu et al., 2010). However, the DIP wood that contains around 11% of extractives showed higher thermal stability than ITA. This behavior may be related to the higher content of lignin in DIP relative to that of ITA and the higher crystallinity index and crystallite size in this wood, as can be seen in Table 3.

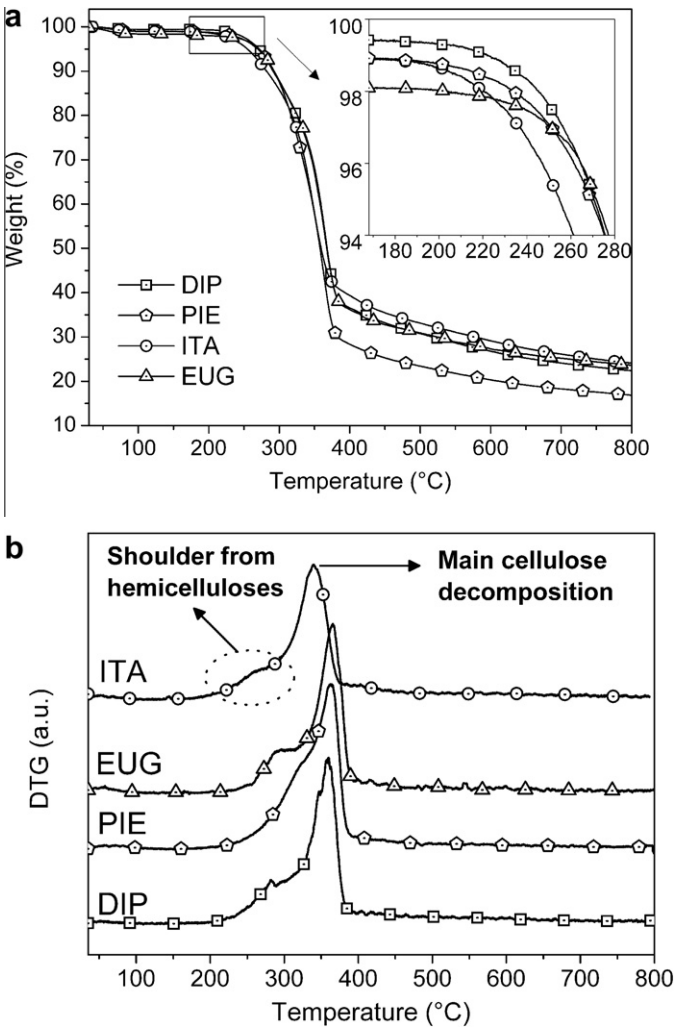

Fig. 3. TGA (a) and DTG (b) curves for the different wood species studied.

Table 4
Thermal degradation temperatures, T shoulder, DTG peak and% residue at 800 °C for the wood species under study.

Wood species	T_i (°C) 3 wt.% loss	T shoulder (°C)	DTG peak (°C)	Residue at 800 °C (%)
Eucalyptus grandis (EUG)	250	291	364	23.6
Pinus elliottii (PIE)	251	322	367	16.8
Dipteryx *odorata* (DIP)	257	289	368	22.4
Mezilaurus itauba (ITA)	237	275	350	24.1

The initial weight loss temperature, T_i, of all samples, is considered as the temperature at which the sample loses 3% of its weight, as showed in Table 4. The lowest T_i value was attributed to ITA, as can be seen in detail in Fig. 3(a). This might be associated with higher volatility of extractives and hemicellulose in this wood. The highest T_i values were observed for the EUG, PIE and DIP wood species. On the other hand, EUG, ITA and DIP had a significant amount of residue at 800 °C probably due to higher inorganic contents in these three wood species.

Wood is commonly used as filler only in polymers that are processed at temperatures at around 200 °C (Araújo et al., 2008; Shebani et al., 2009). Accounting to this fact, the detail in Fig. 3(a) showed that ITA and PIE woods initiate a more pronounced degradation process at around 180–190 °C and 190–200 °C, respectively. The low degradation temperature of ITA and PIE samples can lead to undesirable composite properties, such as browning and decreasing of the mechanical strength when processed at temperatures above 200 °C. On the other hand, DIP and EUG woods initiate a more pronounced degradation process at around 220 °C which can lead to thermoplastic polymer composites with higher mechanical and thermal properties by increasing the processing temperature range.

Because the temperature intervals of hemicellulose, cellulose and lignin decomposition partially overlap each other, the hemicellulose and/or amorphous cellulose decomposition step usually appears as a more or less pronounced shoulder instead of a well-defined peak. This shoulder is better evidenced for the ITA, EUG and DIP wood species, as can be seen in Fig. 3(b). For PIE the shoulder occurs at a higher temperature than for the other wood species. This result may be a consequence, on the one hand, of lower extractives volatility and on the other hand, of lower hemicellulose reactivity. The main degradation of cellulose occurs at higher temperatures for EUG, PIE and DIP respectively. For EUG the main degradation temperature of cellulose occurs at 364 °C and might be related to the higher content of holocellulose and lower content of extractives in this wood, see Table 1. The contents of holocellulose and extractives in PIE wood were comparable to those of EUG, however the cellulose main degradation temperature for this wood occurs at 367 °C. One explanation for this fact is the higher PIE cellulose crystallite size at the (1 1 0) crystallographic plane, which may improve thermal stability. The DIP extractives amount is higher while the content of holocellulose is lower than those of EUG and PIE. However, it is interesting to note that the thermal stability was more pronounced and the main decomposition of cellulose was higher for DIP as compared to EUG and PIE. This behavior may be associated with the highest crystalline index and higher crystallite size of cellulose in this wood. In a recent study, Kim et al. (2010b) showed that the thermal decomposition of cellulose shifted to higher temperatures with increasing crystallinity index and crystallite size.

Some models of the cellulose thermal decomposition in wood have been suggested. Kim et al. (2010b) discussed three possible models for thermal decomposition of wood cellulose crystallites: (a) where decomposition preferentially proceeds along the fiber axis; (b) where a crystallite that once starts to decompose undergoes rapid decomposition while the other crystallites remain largely intact, and (c) a combination of the (a) and (b) models. Zickler et al. (2007) studied the thermal decomposition of cellulose in wood at various temperatures by in situ X-ray diffraction using synchrotron radiation. The authors proposed that the thermal decomposition of cellulose in wood occurs mainly via a thermally activated decrease of the fibril cellulose diameter. This decomposition is followed by a random breaking of the cellulose fibrils into shorter length pieces as a consequence of the extremely anisotropic nature of the higher hydrogen bonding forces in cellulose crystallites (Zickler et al., 2007). As a result, a higher amount of hydrogen bond between neighboring cellulose chains may be resulted from a more packed cellulose structure which can lead out to higher crystallinity and thermal stability, as observed in the case of DIP sample. In addition, intramolecular hydrogen bonds stabilize the cellulose molecules and may inhibit thermal expansion along this direction (Hidaka et al., 2010) improving the wood thermal stability.

Although the decomposition of wood is a complex process and involves a series of competitive and/or consecutive reactions. It might be difficult to distinguish and model the thermal decomposition behavior of each specific component in wood due to the complexity of growth of wood which causes variance in components content, crystal structure and chemical composition from one species to another (Poletto et al., 2010; Yao et al., 2008; Di Blasi, 2008).

4. Conclusions

Chemical analysis reveals that DIP and ITA contain higher amount of extractives than EUG and PIE. The X-ray diffractometry results showed that DIP and ITA contain much more cellulose chains in highly organized form in the interior of the crystallite, which can lead to higher crystallinity. The combined results showed that higher extractives contents associated with lower crystallinity and lower crystallite size accelerate the degradation process and reduce wood thermal stability. However, thermal decomposition of DIP shifted to higher temperatures with increasing cellulose crystallinity and crystallite size. These results indicated that cellulose crystallite size affects the wood thermal degradation temperature.

Acknowledgement

The authors are grateful to Prof. Ricardo Campomanes from Universidade Federal de Mato Grosso (UFMT) for supplying the wood samples and CAPES for financial support.

References

Araújo, J.R., Waldman, W.R., De Paoli, M.A., 2008. Thermal properties of high density polyethylene composites with natural fibres: coupling agent effect. Polym. Degrad. Stab. 93, 1770–1775.
Ashori, A., Nourbakhsh, A., 2010. Reinforced polypropylene composites: effects of chemical compositions and particle size. Bioresour. Technol. 101, 2515–2519.
Branca, C., Albano, A., Di Blasi, C., 2005. Critical evaluation of global mechanisms of wood devolatilization. Thermochim. Acta 429, 133–141.
Branca, C., Di Blasi, C., 2003. Global kinetics of Wood char devolatilization and combustion. Energy Fuels 17, 1609–1615.

Davidson, T.C., Newman, R.H., Ryan, M.J., 2004. Variations in the fibre repeat between samples of cellulose I from different sources. Carbohydr. Res. 339, 2889–2893.

Di Blasi, C., 2008. Modeling chemical and physical process of wood and biomass pyrolysis. Prog. Energy Combust. Sci. 34, 47–90.

Grønli, M.G., Várhegyi, G., Di Blasi, C., 2002. Thermogravimetric analysis and devolatilization kinetics of wood. Ind. Eng. Chem. Res. 41, 4201–4208.

Gümüskaya, E., Usta, M., Kirei, H., 2003. The effects of various pulping conditions on crystalline structure of cellulose in cotton linters. Polym. Degrad. Stab. 81, 559–564.

Hidaka, H., Kim, U.-J., Wada, M., 2010. Synchrotron X-ray fiber diffraction study on the thermal expansion behavior of cellulose crystals in tension wood of Japanese poplar in the low-temperature region. Holzforschung 64, 167–171.

Hon, D.N.-S., Shiraishi, N., 2001. Wood and Cellulosic Chemistry. Marcel Dekker, Inc., New York.

Howell, C.L., 2008. Understanding wood biodegradation through the characterization of crystalline cellulose nanostructures. Doctoral thesis. University of Maine.

John, M.J. & Thomas, S.,2008. Biofibres and biocomposites. Carbohydr. Polym. 71, 343–364.

Kim, S.-S., Kim, J., Park, Y.-H., Park, Y.-K., 2010a. Pyrolysis kinetics and decomposition characteristics of pine trees. Bioresour. Technol. 101, 9797–9802.

Kim, U.-J., Eom, S.H., Wada, M., 2010b. Thermal decomposition of native cellulose: influence on crystallite size. Polym. Degrad. Stab. 95, 778–781.

Kim, H.-S., Kim, S., Kim, H.-J., Yang, H.-S., 2006. Thermal properties of bio-flour-filled polyolefin composites with different compatibilizing agent type and content. Thermochim. Acta 451, 181–188.

Klyosov, A.A., 2007. Wood-Plastic Composites. John Wiley & Sons, Inc., New Jersey.

Liu, H., Wu, Q., Zhang, Q., 2009. Preparation and properties of banana fiber-reinforced composites based on high density polyethylene (HDPE)/Nylon-6 blends. Bioresour. Technol. 100, 6088–6097.

Nachtigall, S.M.B., Cerveira, G.S., Rosa, S.M.L., 2007. New polymeric-coupling agent for polypropylene/wood-flour composites. Polym. Test. 26, 619–628.

Nada, A.-A.M.A., Kamel, S., El-Sakhawy, M., 2000. Thermal behavior and infrared spectroscopy of cellulose carbamates. Polym. Degrad. Stab. 70, 347–355.

Newman, R.H., 2008. Simulation of X-ray diffractograms relevant to the purported polymorphs cellulose IV_I and IV_{II}. Cellulose 15, 769–778.

Newman, R.H., 1999. Estimation of the lateral dimensions of cellulose crystallites using ^{13}C NMR signal strengths. Solid State Nucl. Magn. Reson. 15, 21–29.

Órfão, J.J.M., Antunes, F.J.A., Figueiredo, J.L., 1999. Pyrolysis kinetics of lignocellulosic materials – three independent reactions moldel. Fuel 78, 349–358.

Órfão, J.J.M., Figueiredo, J.L., 2001. A simplified method for determination of lignocellulosic materials pyrolysis kinetics from isothermal thermogravimetric experiments. Thermochim. Acta 380, 67–78.

Poletto, M., Dettenborn, J., Zeni, M., Zattera, A.J., 2011a. Characterization of composites based on expanded polystyrene wastes and wood flour. Waste Manage. 31, 779–784.

Poletto, M., Pistor, V., Zeni, M., Zattera, A.J., 2011b. Crystalline properties and decomposition kinetics of cellulose fibers in wood pulp obtained by two pulping process. Polym. Degrad. Stab. 96, 679–685.

Poletto, M., Dettenborn, J., Pistor, V., Zeni, M., Zattera, A.J., 2010. Materials produced from plant biomass. Part I: evaluation of thermal stability and pyrolysis of wood. Mat. Res. 13, 375–379.

Popescu, C.-M., Popescu, M.-C., Vasile, C., 2010. Structural changes in biodegradable lime wood. Carbohydr. Polym. 79, 362–372.

Popescu, M.-C., Popescu, C.-M., Lisa, G., Sakata, Y., 2011. Evaluation of morphological and chemical aspects of different wood species by spectroscopy and thermal methods. J. Mol. Struct. 988, 65–72.

Rowell, R., 2005. Handbook of Wood Chemistry and Wood Composites. CRC Press, Boca Raton.

Segal, L., Creely, L., Martin, A.E., Conrad, C.M., 1959. An empirical method for estimaring the degree of crystallinity of native cellulose using X-ray diffractometer. Text. Res. J. 29, 786–794.

Shebani, A.N., van Reenen, A.J., Meincken, M., 2009. The effect of wood extractives on the thermal stability of different wood-LLDPE composites. Thermochim. Acta 481, 52–56.

Shebani, A.N., van Reenen, A.J., Meincken, M., 2008. The effect of wood extractives on the thermal stability of different wood species. Thermochim. Acta 471, 43–50.

Shen, D.K., Gu, S., 2009. The mechanism for thermal decomposition of cellulose and its main products. Bioresour. Technol. 100, 6496–6504.

Wada, M., Okano, T., 2001. Localization of I_α and I_β phases in algal cellulose revealed by acid treatments. Cellulose 8, 183–188.

Wada, M., Okano, T., Sugiyama, J., 2001. Allomorphs of native crystalline cellulose I evaluated by two equatorial d-spacings. J. Wood Sci. 47, 124–128.

Wongsiriamnuay, T., Tippayawong, N., 2010. Non-isothermal pyrolysis characteristics of giant sensitive plants using thermogravimetric analysis. Bioresour. Technol. 101, 5638–5644.

Yao, F., Wu, Q., Lei, Y., Guo, W., Xu, Y., 2008. Thermal decomposition kinetics of natural fibers: Activation energy with dynamic thermogravimetric analysis. Polym. Degrad. Stab. 93, 90–98.

Yang, H., Yan, R., Chen, H., Zheng, C., Lee, D.H., Liang, D.T., 2006. In-depth investigation of biomass pyrolysis based on three major components: hemicellulose, cellulose and lignin. Energy Fuels 20, 388–393.

Zickler, G.A., Wagermaier, W., Funari, S.S., Burghammer, M., Paris, O., 2007. *In situ* X-ray diffraction investigation of thermal decomposition of wood cellulose. J. Anal. Appl. Pyrolysis 80, 134–140.